

# Study phase evolution of hydrothermally synthesized $\text{Cu}_2\text{ZnSnS}_4$ nanocrystals by Raman spectroscopy

Thi Ha Tran<sup>a</sup>, Thi Hong Pham<sup>b</sup>, Cong Doanh Sai<sup>b,\*</sup>, Trong Tam Nguyen<sup>c</sup>, Viet Tuyen Nguyen<sup>b,\*</sup>

<sup>a</sup> Faculty of Basic Sciences, Hanoi University of Mining and Geology, Duc Thang, Tu Liem, Hanoi, Viet Nam

<sup>b</sup> Faculty of Physics, Vietnam National University Hanoi, University of Science, 334 Nguyen Trai, Thanh Xuan, Hanoi, Viet Nam

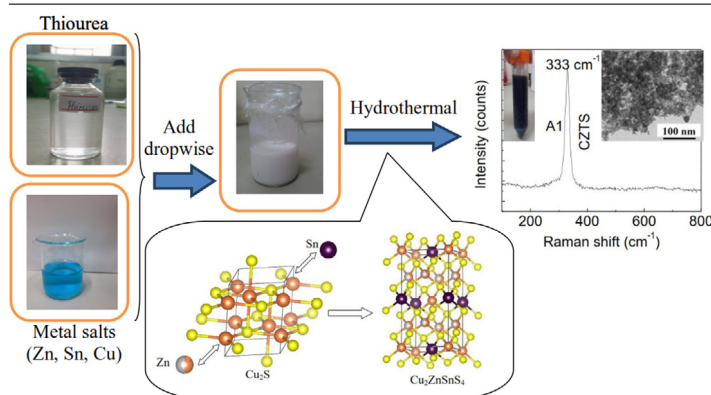
<sup>c</sup> Department of Physics, Faculty of Basic –Fundamental Sciences, Vietnam Maritime University, 484 Lach Tray – Le Chan - Hai Phong, Viet Nam



## HIGHLIGHTS

- $\text{Cu}_2\text{ZnSnS}_4$  nanoparticles were synthesized by single step hydrothermal method.
- Hydrothermal temperature and time are critical to the formation of single phase  $\text{Cu}_2\text{ZnSnS}_4$  nanoparticles.
- Raman data suggested that  $\text{Cu}_2\text{S}$  was formed first, Sn and Zn ion were incorporated in the next stage to form  $\text{Cu}_2\text{ZnSnS}_4$ .

## GRAPHICAL ABSTRACT



## ARTICLE INFO

### Article history:

Received 12 November 2018

Received in revised form 26 December 2018

Accepted 22 February 2019

### Keywords:

Hydrothermal

Kesterite

Nanocrystals

Solar cells

$\text{Cu}_2\text{ZnSnS}_4$

## ABSTRACT

$\text{Cu}_2\text{ZnSnS}_4$  (CZTS) is a p-type semiconductor with kesterite/stannite structure. CZTS has band gap of about 1.0–1.5 eV, and a high absorption coefficient (over  $10^4 \text{ cm}^{-1}$ ), which is ideal for making absorber layer in solar cells. CZTS is only composed of abundant earth and environment friendly elements so this material can contribute to the sustainable development of photovoltaic field and to reducing the cost of solar cells. Hydrothermal method, with many advantages such as simplicity, cost saving, was used to produce CZTS material in this research. Raman scattering, X-ray diffraction, transmission electron microscopy, and energy dispersive X-ray spectroscopy show that the products are nanocrystals of kesterite phase with uniform size distribution. The chemical pathway for the formation of kesterite phase was also discussed based on Raman results.

© 2019 Elsevier B.V. All rights reserved.

## 1. Introduction

The development of new light absorbing materials for applications in photovoltaic (PV) technologies is driven by necessity to overcome the key issues in the current PV technologies. The first

generation of solar cells consists mainly of single crystal silicon which offers good light absorption spectrum with small internal resistance. However, high manufacturing cost, complex processes of growing and cutting silicon wafers limited the ability to reduce the price of producing electricity. The second generation solar cell is thin film solar cell, which includes two or three elements such as CdTe or  $\text{CuInS}_2$  (CIS) [1,2]. The second type of solar cell has shown the potential for improving performance of solar cells at lower price. Thin films solar cells based on four-elements

\* Corresponding authors.

E-mail addresses: [saidoanh@hus.edu.vn](mailto:saidoanh@hus.edu.vn) (C.D. Sai), [nguyenvietuyen@hus.edu.vn](mailto:nguyenvietuyen@hus.edu.vn) (V.T. Nguyen).

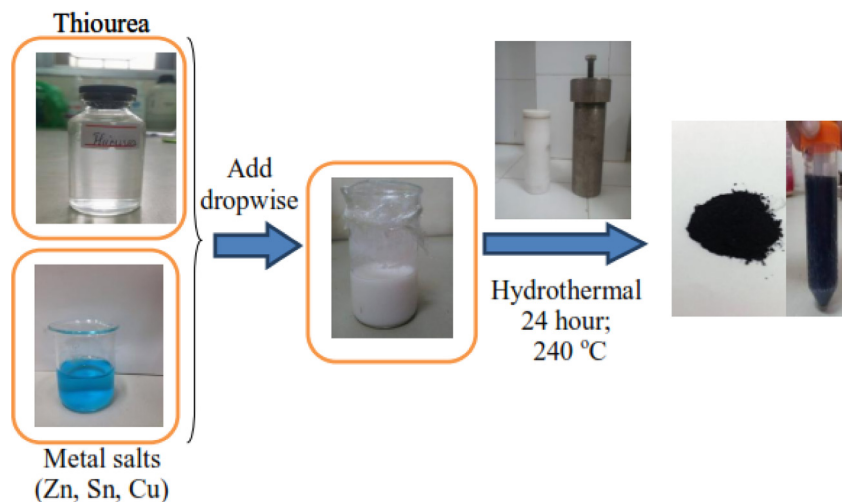


Fig. 1. Schematic diagram of CZTS nanoparticle preparation.

materials such as  $\text{Cu}(\text{In, Ga})(\text{S,Se})_2$  (CIGS) have achieved energy conversion efficiency of about 20% or higher [3–6] but high cost of rare elements like Indium and Gallium offers no prospects for commercialization.

Recently, CZTS is widely studied as a promising replacement for CIGS. CZTS is a p-type semiconductor and with direct band gap of around 1.5 eV, and a high absorption coefficient (over  $10^4 \text{ cm}^{-1}$ ). The characteristics are ideal for photovoltaic applications [7–10]. CZTS is composed only of abundantly available in the Earth's crust, environment friendly and low cost elements. CZTS has three structures: kesterite (KS), stannite (ST), primitive mixed Cu-Au (PMCA) and kesterite is the most common phase.

In the ternary phase diagram of  $\text{Cu}_2\text{S}$ - $\text{SnS}$ - $\text{ZnS}$  system, CZTS exists only in a small region, which means that the secondary phases such as  $\text{CuS}$ ,  $\text{ZnS}$ ,  $\text{SnS}_2$  are more favorable and make it quite difficult to get pure phase CZTS [11–13]. All of these secondary phases if any will degrade the absorber layer because they can provide shunting current paths through the solar cell, act as recombination centers or increase the series resistance of the cell. So investigating how to control the formation of such secondary phases is extremely important. In this paper, CZTS was prepared by hydrothermal method, which shows many advantages such as simplicity, cost saving. By controlling some parameters such as hydrothermal time, hydrothermal temperature, CZTS of pure phase was obtained. Furthermore, the Raman data for sample prepared in different duration reveals the chemical pathway for the formation of CZTS phase, which provides very useful information for better understanding the growth of CZTS by chemical process.

## 2. Experiment

The starting chemicals which are copper (II) sulfate pentahydrate ( $\text{Cu}_2\text{SO}_4 \cdot 5\text{H}_2\text{O}$ ), zinc sulfate heptahydrate ( $\text{ZnSO}_4 \cdot 7\text{H}_2\text{O}$ ), tin chloride pentahydrate ( $\text{SnCl}_4 \cdot 5\text{H}_2\text{O}$ ), thiourea ( $\text{CH}_4\text{N}_2\text{S}$ ) were purchased from Merk, Germany, all of analytical grade and used without further purification.

In a typical experimental procedure, equal volumes of 10 ml of 0.4 M  $\text{Cu}_2\text{SO}_4 \cdot 5\text{H}_2\text{O}$ , 0.2 M  $\text{ZnSO}_4 \cdot 7\text{H}_2\text{O}$ , and 0.2 M  $\text{SnCl}_4 \cdot 5\text{H}_2\text{O}$  were mixed together by using magnetic stirrer. 10 ml of 1.35 M thiourea was then added drop wise to the above salt mixture solution. The resulted solution was stirred for 20 min to obtain a milky color solution. In the next step, the precursor solution was transferred into a teflon bottle to perform hydrothermal reaction at three different temperatures: 120 °C, 180 °C, 240 °C and in different durations: 6 h, 12 h, 24 h to study the effect

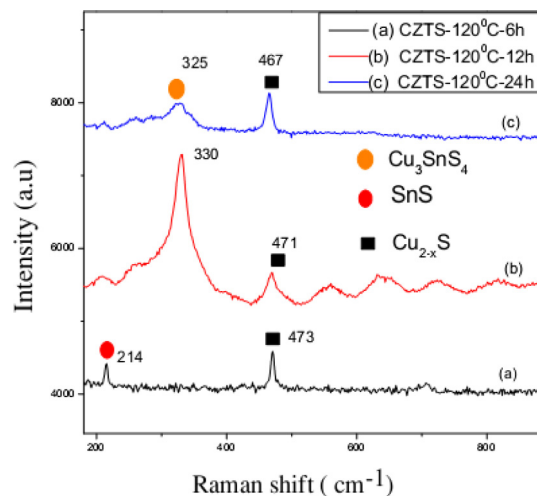


Fig. 2. Raman spectra of samples prepared at 120 °C in different time: (a) 6 h; (b) 12 h; (c) 24 h.

of these parameters on the product. The obtained products were washed at least five times with distilled water and ethanol by centrifugation at 5000 rpm in 20 min for one cycle. Then the products were dried at 65 °C during 7 h, final products was obtained in form of black powder (see Fig. 1).

## 3. Results and discussion

While X-ray diffraction pattern cannot resolve peaks of different secondary phases from those of CZTS due to the similar scattering cross section area, Raman scattering is very effective to detect secondary phases that could occur in CZTS. Raman spectrum of sample prepared at 120 °C in 6 h, shown in Fig. 2, is composed of a strong peak at  $473 \text{ cm}^{-1}$  corresponding to vibration of  $\text{Cu}_{2-x}\text{S}$  and a lower peak at  $214 \text{ cm}^{-1}$  belonging to  $\text{SnS}$ . Raman spectrum of sample prepared in 12 h shows one peak at  $471 \text{ cm}^{-1}$  of  $\text{Cu}_{2-x}\text{S}$  and a strong  $A_1$  peak at  $330 \text{ cm}^{-1}$  of CZTS. When reaction time increases to 24 h, Raman spectrum is dominated by two peaks, one at  $325 \text{ cm}^{-1}$  of  $\text{Cu}_3\text{SnS}_4$  phase and the other at  $467 \text{ cm}^{-1}$  of  $\text{Cu}_{2-x}\text{S}$ .

Fig. 3 shows Raman spectra of samples prepared at 180 °C in different durations, 6, 12 and 24 h. All Raman spectra show two peaks at  $331\text{--}333 \text{ cm}^{-1}$  and  $469\text{--}472 \text{ cm}^{-1}$ , which are typical

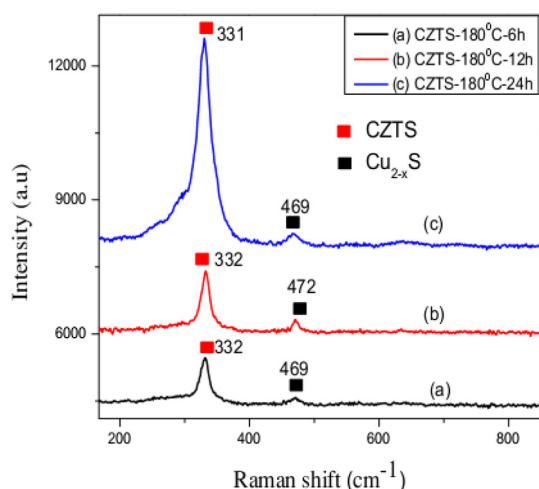


**Fig. 3.** Raman spectra of samples prepared at 180 °C in different time: (a) 6 h; (b) 12 h; (c) 24 h.

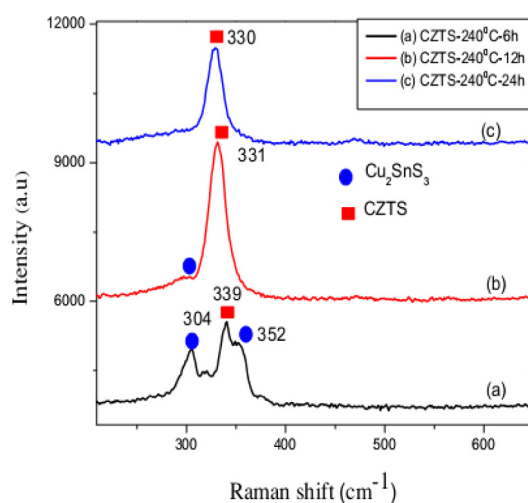


**Fig. 4.** Raman spectra of samples prepared at 240 °C in 6, 12 and 24 h.

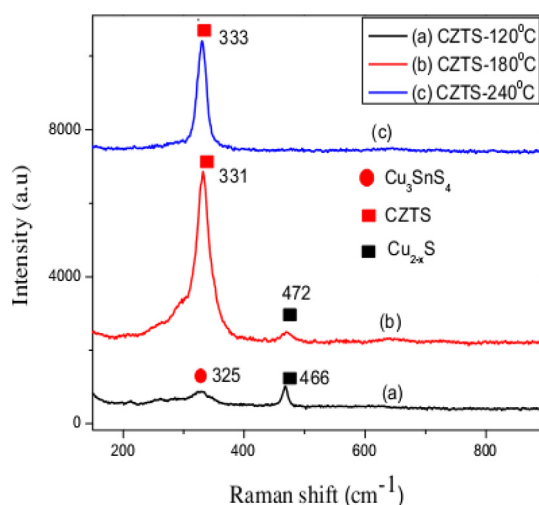


**Fig. 5.** Raman spectra of samples prepared at different temperatures when hydrothermal time was kept constant at 24 h.

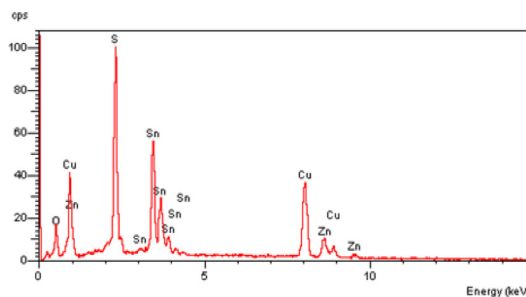


**Fig. 6.** EDS Spectrum of CZTS sample prepared at 240 °C in 24 h.

peaks of CZTS and  $\text{Cu}_{2-x}\text{S}$  respectively. At 180 °C, CZTS was formed as the main product, however, the existence of  $\text{Cu}_{2-x}\text{S}$  even at a low concentration could degrade the efficiency of the cell, so a higher hydrothermal temperature at 240 °C was investigated. Fig. 4 shows Raman spectra of samples prepared at 240 °C in 6, 12 and 24 h.

At 240 °C,  $\text{Cu}_2\text{SnS}_3$  was formed first and dominated at the first stage of the reaction. As the reaction time was prolonged, this phase gradually transformed into CZTS, and after 24 h, a pure phase of CZTS was obtained as the final product.

Based on the Raman results, it can be understood that a temperature lower than 240 °C or a reaction time less than 24 h is not enough to convert the precursors into CZTS and results in the formation of  $\text{Cu}_{2-x}\text{S}$  or  $\text{Cu}_2\text{SnS}_3$  as secondary phases (Fig. 5).

Energy-dispersive spectroscopy was used for the elemental analysis of the CZTS sample prepared at 240 °C and in 24 h, and the result is shown in Fig. 6. The sample is only composed of Cu, Zn, Sn, and S elements. The elemental percentage of Cu:Zn:Sn:S is 28.18:15.83:13.16:42.83, quite close to the stoichiometry value.

From the above results, we suggested the following growth process of CZTS.  $\text{Cu}_{2-x}\text{S}$  was first formed during the hydrothermal reaction.  $\text{Sn}^{4+}$  cations were then incorporated into the crystal lattice of  $\text{Cu}_{2-x}\text{S}$  and replaced  $\text{Cu}^+$  to form  $\text{Cu}_2\text{SnS}_3$  or  $\text{Cu}_3\text{SnS}_4$ , and finally  $\text{Zn}^{2+}$  went inside to create CZTS in the hydrothermal process.

The XRD pattern of the sample is shown in Fig. 7(a). All diffraction peaks match well with the JCPDS of kesterite CZTS. Prominent peaks can be observed at 28.4°, 33.9°, 47.4°, 56.3° which correspond to the reflections from (112), (200), (220)/(204) and (312) planes, respectively.

The lattice constants determined from the XRD patterns are  $a = b = 5.4 \text{ \AA}$ ,  $c = 10.9 \text{ \AA}$ , which are in good agreement with the reported value for the kesterite structure of CZTS [14]. The average size of the crystallites was estimated by the Debye–Scherrer's formula [10]:

$$D = \frac{0.9\lambda}{\beta \cos \theta}$$

where  $\beta$  is the full width at half maximum (FWHM) in radians of the diffraction peaks,  $\theta$  is the Bragg's diffraction angle, and  $\lambda = 1.54 \text{ \AA}$  is the wavelength of  $\text{Cu K}\alpha$  radiation used in the diffractometer. The average crystal size is 16 nm.

TEM image of CZTS nanopowder prepared at 240 °C in 24 h is shown in Fig. 7b. CZTS nanoparticles have a quasi-spherical shape and loosely aggregate to form clusters. The average size of these nanoproductions ranges from 10–25 nm.

#### 4. Conclusion

We have successfully prepared CZTS material by the hydrothermal method. CZTS product, obtained at 240 °C in 24 h, is a single phase, uniform in size. The Raman data shows that the formation of  $\text{Cu}_{2-x}\text{S}$  and the diffusion of  $\text{Sn}^{4+}$  and  $\text{Zn}^{2+}$  ions into the crystal lattice

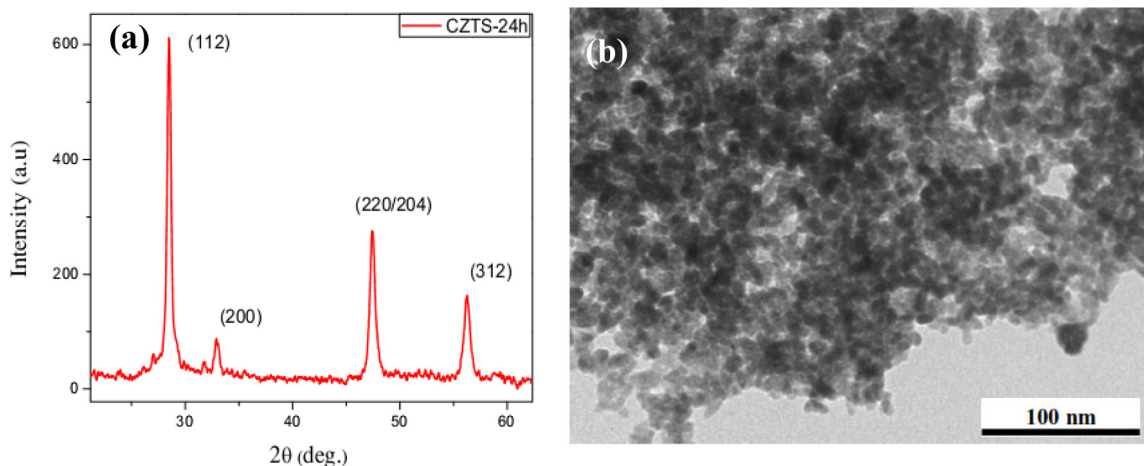


**Fig. 7.** XRD pattern (a) and TEM image (b) of CZTS sample synthesized at 240 °C in 24 h.

of  $\text{Cu}_{2-x}\text{S}$  results in the growth of CZTS. The successful synthesis of CZTS material by hydrothermal method indicates the promise of this material for application in low cost thin film solar cells.

### Acknowledgments

The author would like to thank Faculty of Physics, VNU University of Science for letting use the equipment.

### Conflict of interest

The authors declare that there is no conflict of interest.

### References

- [1] Z.-B.K. Gutierrez, P.G. Zayas-Bazán, O. Melo, F. Moure-Flores, J.A. Andraca-Adame, L.A. Moreno-Ruiz, H. Martínez-Gutiérrez, S. Gallardo, J. Sastré-Hernández, G. Contreras-Puente, CdS/CdTe Heterostructures for applications in ultra-thin solar cells, *Materials* 11 (2018) 1788(1)–1788(8), <http://dx.doi.org/10.3390/ma11101788>.
- [2] N. Tsolekile, S. Parani, M.C. Matoetoe, S.P. Songca, O.S. Oluwafemi, Evolution of ternary I–III–VI QDs: Synthesis, characterization and application, *Nano-Struct. Nano-Objects* 12 (2017) 46–56, <http://dx.doi.org/10.1016/j.nanoso.2017.08.012>.
- [3] C. Malerba, F. Biccari, C.L.A. Ricardo, M. Valentini, R. Chierchia, M. Müller, A. Santoni, E. Esposito, P. Mangiapane, P. Scardi, A. Mittiga, CZTS Stoichiometry effects on the band gap energy, *J. Alloy. Compd.* 582 (2014) 528–534, <http://dx.doi.org/10.1016/j.jallcom.2013.07.199>.
- [4] N. Ali, R. Ahmed, B.-U. Haq, A. Shaari, *Advances in CZTS thin films and nanostructured*, *Opto-Electron. Rev.* 23 (2) (2015) 137–142, <http://dx.doi.org/10.1515/oere-2015-0022>.
- [5] S. Zhuka, A. Kushwahaa, T.K.S. Wongb, S.M. Panaha, A. Smirnovd, G.K. Dalapatia, Critical review on sputter-deposited  $\text{Cu}_2\text{ZnSnS}_4$  (CZTS) based thin film photovoltaic technology focusing on device architecture and absorber quality on the solar cells performance, *Sol. Energy Mater. Sol. Cells* 171 (2017) 239–252, <http://dx.doi.org/10.1016/j.solmat.2017.05.064>.
- [6] M. Singh, P. Prasher, K. Suganuma, Fabrication of dense CIGS film by mixing two types of nanoparticles for solar cell application, *Nano-Struct. Nano-Objects* 11 (2017) 129–134, <http://dx.doi.org/10.1016/j.nanoso.2017.08.002>.
- [7] J. Zhong, Z. Xia, M. Luo, J. Zhao, J. Chen, L. Wang, X. Liu, D.-J. Xue, Y.-B. Cheng, H. Song, J. Tang, Sulfurization induced surface constitution and its correlation to the performance of solution-processed  $\text{Cu}_2\text{ZnSn}(\text{S}, \text{Se})_4$  solar cells, *Sci. Rep.* 4 (2014) 6288(1)–6288(9), <http://dx.doi.org/10.1038/srep06288>.
- [8] C.-L. Wang, C.-C. Wang, B. Rejea-Jayan, A. Manthiram, Low-cost, S. Mo-, Low-cost,  $\text{Mo}(\text{S}, \text{Se})_2$ -free superstrate-type solar cells fabricated with tunable band gap  $\text{Cu}_2\text{ZnSn}(\text{S}_{1-x}\text{Se}_x)_4$  nanocrystal-based inks and the effect of sulfurization, *RSC Adv.* 3 (2013) 19946–19951, <http://dx.doi.org/10.1039/C3RA42624F>.
- [9] M.P. Suryawanshi, U.V. Ghorpade, U.P. Suryawanshi, M. He, J. Kim, M.G. Gang, P.S. Patil, A.V. Moholkar, J.H. Yun, J.H. Kim, Aqueous solution processed  $\text{Cu}_2\text{ZnSn}(\text{S}, \text{Se})_4$  thin film solar cells via an improved successive ion layer adsorption reaction sequence, *ACS Omega* 2 (2017) 9211–9220, <http://dx.doi.org/10.1021/acsomega.7b00967>.
- [10] I.D. Olekseyuk, I.V. Dudchak, L.V. Piskach, Phase equilibria in the  $\text{Cu}_2\text{S}-\text{ZnS}-\text{SnS}_2$  system, *J. Alloy. Compd.* 368 (2003) 135–143, <http://dx.doi.org/10.1016/j.jallcom.2003.08.084>.
- [11] P.A. Fernandes, P.M.P. Salomé, A.F. da Cunha, Study of polycrystalline  $\text{Cu}_2\text{ZnSnSe}_4$  films by Raman scattering, *J. Alloy. Compd.* 509 (2011) 7600–7606, <http://dx.doi.org/10.1016/j.jallcom.2011.04.097>.
- [12] S. Jain, P. Chawla, S.N. Sharma, D. Singh, N. Vijayan, Efficient colloidal route to pure phase kesterite  $\text{Cu}_2\text{ZnSnS}_4$  (CZTS) nanocrystals with controlled shape and structure, *Superlattices Microstruct.* 119 (2018) 59–71, <http://dx.doi.org/10.1038/srep06288> [10.1038/srep06288].
- [13] Viet Tuyen Nguyen, Dahyun Nam, Mungunshagai Gansukh, Si-Nae Park, Shi-Joon Sung, Dae-Hwan Kim, Jin-Kyu Kang, Cong Doanh Sai, Thi Ha Tran, Hyeonsik Cheong, Influence of sulfate residue on  $\text{Cu}_2\text{ZnSnS}_4$  thin films prepared by direct solution method, *Sol. Energy Mater. Sol. Cells* 136 (2015) 113–119, <http://dx.doi.org/10.1016/j.solmat.2015.01.003>.
- [14] T. Shiyani, D. Raval, M. Patel, I. Mukhopadhyay, A. Ray, Effect of annealing on structural properties of electrodeposited CZTS thin films, *Mater. Chem. Phys.* 171 (2016) 63–72, <http://dx.doi.org/10.1080/02564602.2015.1045044>.